Remote Sensing of Environment 140 (2014) 14–22

Contents lists available at ScienceDirect

Remote Sensing of Environment

journal homepage: www.elsevier.com/locate/rse

Year-to-year salinity changes in the Amazon plume: Contrasting 2011 and 2012 Aquarius/SACD and SMOS satellite data

Semyon A. Grodsky [a,*], Gilles Reverdin [b], James A. Carton [a], Victoria J. Coles [c]

[a] Department of Atmospheric and Oceanic Science, University of Maryland, College Park, MD, USA
[b] Laboratoire d'Océanographie et de Climatologie par Expérimentation et Analyse Numérique, Institut Pierre Simon Laplace, CNRS/UPMC/IRD/MNHN, Paris, France
[c] University of Maryland Center for Environmental Science, Horn Point Laboratory, Cambridge, MD, USA

ARTICLE INFO

Article history:
Received 29 May 2013
Received in revised form 5 August 2013
Accepted 12 August 2013
Available online 19 September 2013

Keywords:
Satellite salinity
Amazon plume
Interannual variability

ABSTRACT

The fresh Amazon/Orinoco plume covers in excess of 10^6 km^2 in late summer–early fall forming a near-surface barrier layer that reduces exchange with the cooler, saltier water below. Barrier layers and higher water turbidity keep SST in the region high and thus are factors in the development of fall season hurricanes. Year to year changes in key properties of salinity and areal coverage may depend on a number of factors including river discharge, ocean rainfall, vertical entrainment rate, and horizontal advection. This study uses new sea surface salinity observations from the Aquarius/SACD and SMOS satellites to show that the plume was 1 psu saltier in early fall 2012 than in the previous fall (despite a stronger Amazon discharge in 2012) and explores the possible causes. The study concludes that the most likely causes of the 2012 salinification are a relative deficit of rainfall over the inflow to the plume region well southeast of the plume in spring and a weaker North Brazil current in spring–summer. The results suggest that tracking spring rainfall can potentially contribute to forecasting the Amazon plume stratification during the fall hurricane season.

1. Introduction

The Amazon/Orinoco plume is a vast seasonal zone of surface water in the western tropical Atlantic with salinities that are several psu fresher than the water beneath the barrier layer (e.g. Lentz, 1995). Recent studies have linked the intensification of hurricanes to the presence of this plume due to the impact of haline stratification on reduction of vertical heat flux (e.g. Balaguru et al., 2012; Ffield, 2007; Grodsky et al., 2012). The seasonal extent of the plume is the result of several competing processes including changes in Amazon River discharge, advection, and turbulent mixing by the strongly seasonal winds (e.g. Hu, Montgomery, Schmitt, & Muller-Karger, 2004; Nikiema, Devenon, & Baklouti, 2007; Zeng et al., 2008). Here we consider the potential role of nonlocal precipitation that changes the properties of the inflow to the region and changing plume advection in contributing to year to year variations in the plume.

The area of the combined Amazon/Orinoco plume, defined as the area covered by water with SSS < 35 psu, reaches its maximum northward and eastward extent in August–September when the zone of weak winds shifts northward. The plume contracts by November, coincident with the reappearance of the northeast trade winds and shifts in the surface currents (Dessier & Donguy, 1994) suggesting that diluted surface water is destratified by the strengthening winds of late fall (e.g. Grodsky et al., 2012). With the exception of rare surveys and thermosalinograph (TSG) observations along commercial shipping lanes the best information on year-to-year variations in the plume has come indirectly from tracking anomalous optical properties associated with coastal water (Hu et al., 2004; Muller-Karger, McClain, & Richardson, 1988; Salisbury et al., 2011; Zeng et al., 2008). These studies have suggested that year to year changes in Amazon River discharge play an important role driving year to year changes in the plume. However, since river discharge strongly affects water optical properties, this approach may only be detecting the portion of the plume associated with river discharge.

The Amazon River discharge varies seasonally from a minimum of 0.8×10^5 m^3 s^{-1} in November to a maximum of 2.4×10^5 m^3 s^{-1} in late May in response to the seasonal southward shift of the intertropical convergence zone (ITCZ, Lentz, 1995). During boreal winter, water in the plume is stored at the river mouth, trapped against the coast by onshore winds. In boreal spring, water in the plume is transported northwestward along the shelf and shelf break by the North Brazil current (NBC). By boreal summer this low salinity surface water is transported mainly by three export pathways (Fig. 1), whose seasonality is discussed by Foltz and McPhaden (2008). Some continue northwestward towards the Caribbean current (Hellweger & Gordon, 2002), some is transported northward by wind-driven Ekman currents and eddies into the barrier layer region east of the Lesser Antilles (Mignot, Lazar, & Lacarra, 2012), and some is carried eastward into the north equatorial counter current (NECC, Carton & Katz, 1990). Indeed, from August through October typically 70% of the Amazon plume water is deflected eastward in the NECC along the NBC retroflection (Lentz, 1995). These three export pathways are seen in the spatial pattern of September

* Corresponding author. Tel.: +1 301 405 5330; fax: +1 301 314 9482.
E-mail address: senya@atmos.umd.edu (S.A. Grodsky).

0034-4257/$ – see front matter © 2013 Elsevier Inc. All rights reserved.
http://dx.doi.org/10.1016/j.rse.2013.08.033

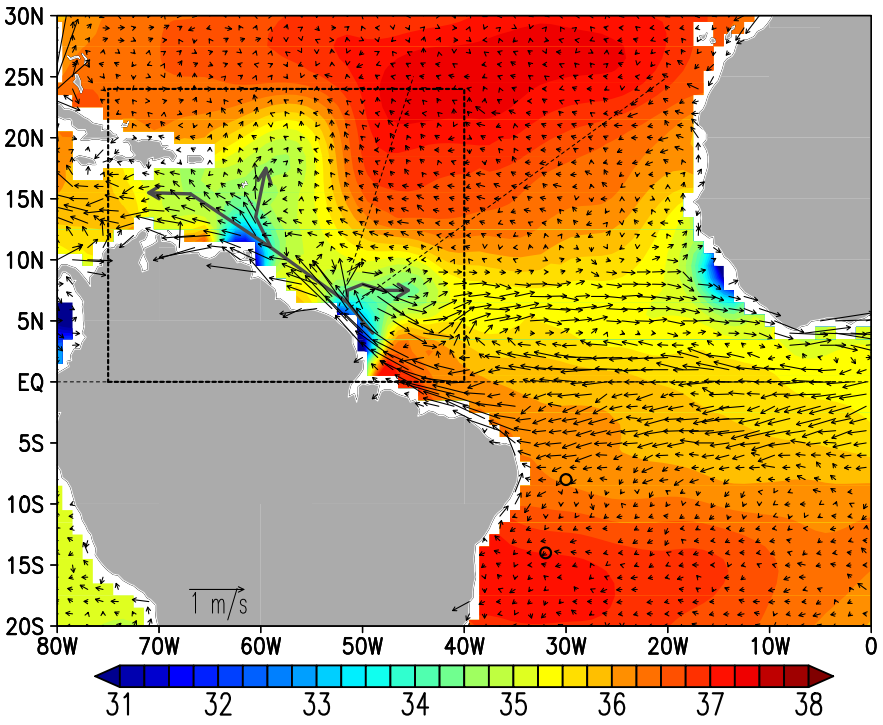

Fig. 1. Climatological September SSS (psu) from the World Ocean Atlas 2009 and June–September climatological surface drifter currents. Bold gray lines illustrate major export pathways of the Amazon waters. Dashed rectangle is the Amazon plume index region. The 8°S, 30°W and 14°S, 32°W PIRATA mooring locations are overlain. Ship of opportunity thermosalinograph transects (discussed in Fig. 2) are located within the directional cone bounded by the two dashed lines.

climatological SSS as low salinity directional lobes extending into the Caribbean, north subtropical Atlantic, and central tropical Atlantic along the NECC (Fig. 1). The Orinoco plume to the northeast also varies seasonally from a minimum of 1×10^4 m^3 s^{-1} in March to a maximum of 7×10^4 m^3 s^{-1} in August (e.g. Hu et al., 2004). The latter plume area may exceed 160,000 km^2 in fall, but much of the Orinoco discharge is swept into the Southern Caribbean Sea. The NBC is the main route by which water is transported into the plume area. This suggests that water characteristics upstream in the South Equatorial Current region that feeds the NBC may impact salinity in the plume through this import pathway.

Interannual anomalies of plume size correlate (0.58) with anomalous Amazon flow at Obidos (Zeng et al., 2008) suggesting a significant impact from the Amazon, but leaving room for other mechanisms to

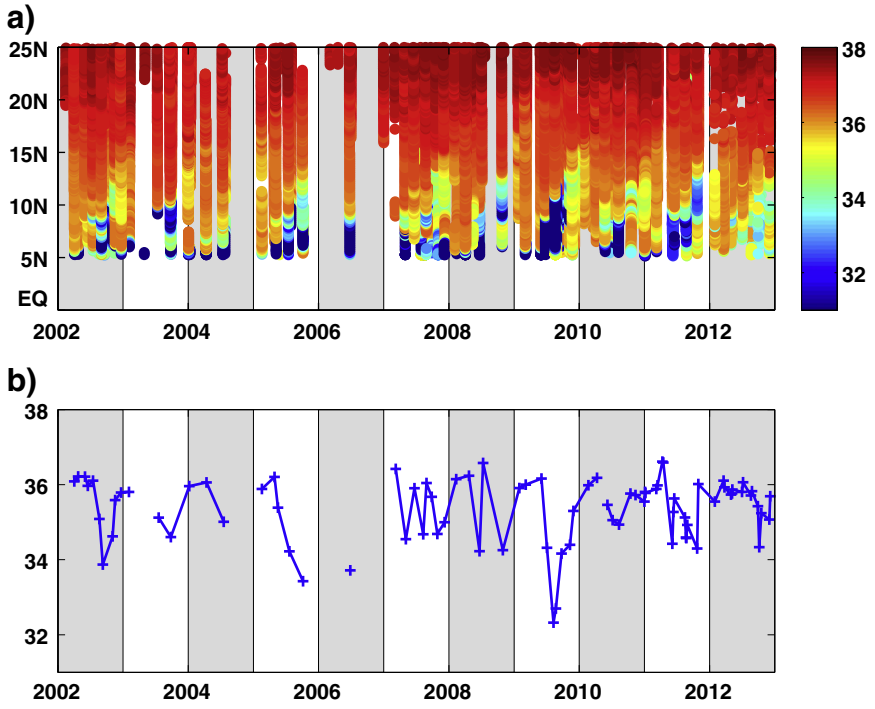

Fig. 2. Ship of opportunity thermosalinograph salinity from transects located within the directional cone bounded by dashed lines in Fig. 1. (a) Salinity with time and latitude. (b) Salinity averaged between 6°N and 15°N along each transect with time. Data are shown only for transects with continuous data coverage in this latitude band.

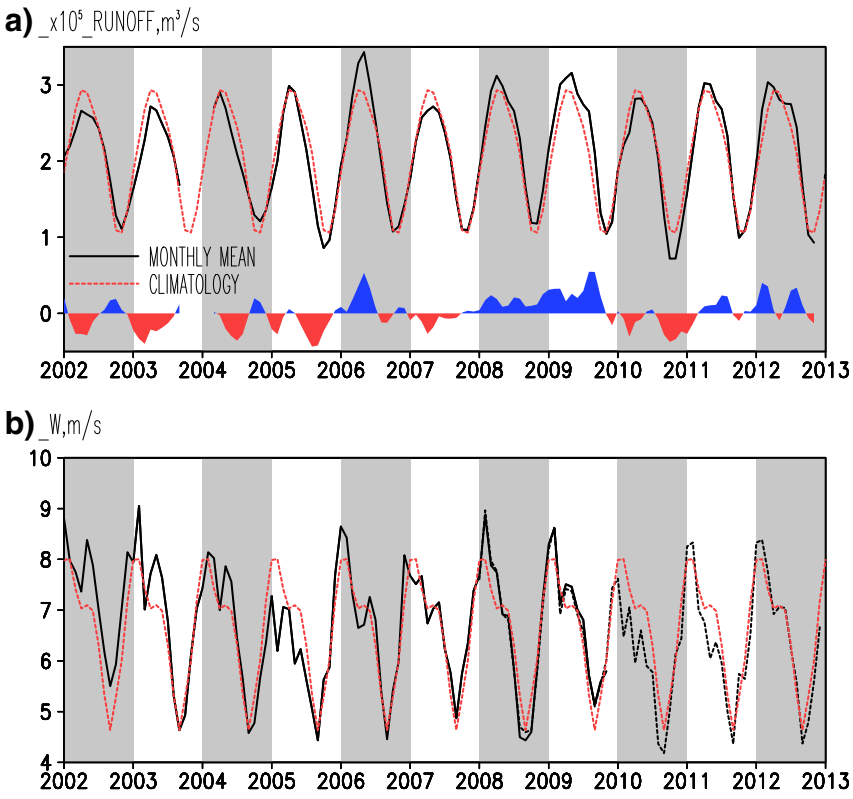

Fig. 3. (a) Combined Amazon–Tocantins River discharge evaluated as a combined discharge of the Amazon River at the Obidos, Tapajos, Xingu, and Tocantins Rivers. Shading is anomalous combined discharge. (b) Wind speed averaged over a portion of the plume index area defined by the area where September climatological SSS < 35 psu (see Fig. 1). QuikSCAT is solid black, ASCAT is dashed black. Monthly mean observations (black), monthly climatology based on the 2002–2012 time span (red dashed) in both panels. The monthly discharge data are provided by the HYBAM observatory and the Brazil Water Agency.

influence plume area. Perhaps this interannual Amazon impact is not surprising since rainfall over the continent (e.g. Ropelewski & Halpert, 1987), and thus Amazon discharge, undergoes interannual and decadal changes including a 10% increase of discharge during La Niña years (e.g. Amarasekera, Lee, Williams, & Eltahir, 1997). In fact 2011 was the second year of the 2010–11 La Niña followed by weak El Nino in early 2012, and thus one might have expected some increase in Amazon discharge in 2011 relative to 2012. But, in fact, the previous year's La Niña conditions resulted in greater upper Amazon flow in 2012 (Satyamurty, da Costa, Manzi, & Candido, 2013) indicating that water storage can cause significant phase lags in the rainfall–discharge relationship (Chen, Wilson, & Tapley, 2010).

Amazon rainfall is also affected by the tropical Atlantic SST (e.g. Xie & Carton, 2004). In particular, one of the strongest Amazon discharge events in recent years, the 2009 flooding (Foltz, McPhaden, & Lumpkin, 2012), was triggered by anomalous cooling of SST in the equatorial north Atlantic and resulted in an anomalous southward shift of the ITCZ, severe flooding in northeast Brazil, and above normal Amazon discharge. Although relative changes in the Amazon discharge are not large (some 10%), their magnitude may well exceed the total discharge by any other Atlantic river.

Because the fresh Amazon/Orinoco plume covers a highly variable area that extends seasonally over 10^6 km^2, the best way to monitor its variability is provided by satellite sensors as has been demonstrated using ocean color data (e.g. Hu et al., 2004). Recently two instruments, the soil moisture and ocean salinity (SMOS) (Boutin, Martin, Reverdin, Yin, & Gaillard, 2013) and the US/Argentina Aquarius/SACD (Lagerloef et al., 2012) have begun providing sea surface salinity (SSS) measurements from space, offering a more direct approach to track the plume characteristics (Tzortzi, Josey, Srokosz, & Gommenginger, 2013). Here we use observations from the Aquarius mission together with ancillary observations to identify a dramatic salinification of the plume from the summer–fall of 2011 to the summer–fall of 2012 and explore the potential causes of this change.

2. Data

The main SSS data set used in this study is the daily level 3 version 2.0 Aquarius SSS beginning 25 August, 2011, obtained from the NASA Jet Propulsion Laboratory Physical Oceanography Distributed Active Archive Center on a 1° × 1° grid. We compare Aquarius SSS with the ESA soil moisture and ocean salinity (SMOS) SSS derived by LOCEAN/IPSL for 2010–2012 (LOCEAN_v2013, reprocessed, Boutin et al., 2013; Yin, Boutin, & Spurgeon, 2012). The observations are known to contain seasonally dependent errors which may exceed 1 psu at high latitudes but are smaller in the tropics (Lagerloef, 2013). We minimize the impact of these seasonal errors by comparing the monthly average SSS for the same month in different years. The satellite SSS is compared to monthly SSS climatology based on in situ observations from the World Ocean Atlas 2009 (Boyer et al., 2012) as well as to concurrent in situ observations.

In this study we consider three sources of in situ salinity observations. The first is the near-surface TSG salinity collected by the Global Ocean Surface Underway Data (GOSUD) Project (www.gosud.org). These data represent salinity at approximately 5 m depth. The second is nearsurface SSS underway observations from two cruises from the Amazon iNfluence on the Atlantic: CarbOn export from Nitrogen fixation by DiAtom Symbioses (ANACONDAS) program: aboard the R/V Melville (MV1110) in August–September, 2011 and the R/V Atlantis (AT21-04) in July–August 2012. The third are salinity time series from

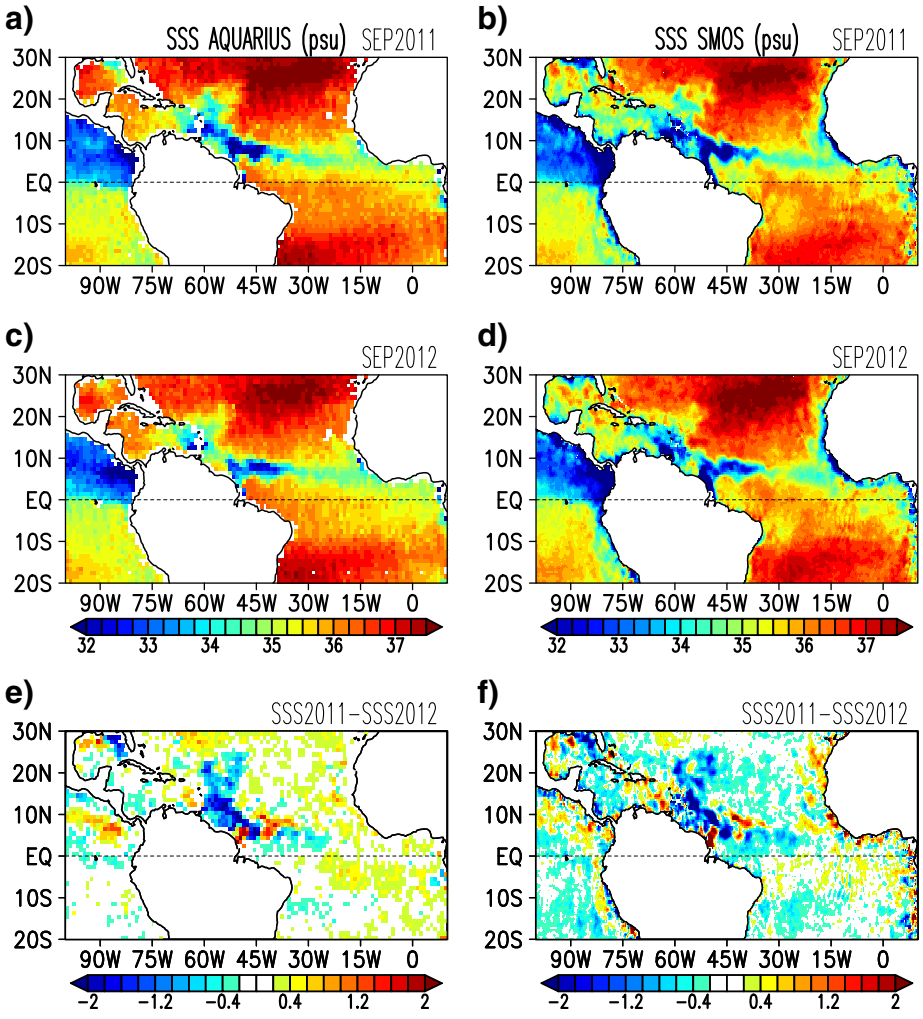

Fig. 4. Aquarius (left) and SMOS (right) SSS averaged September (a,b) 2011, (c,d) 2012, and (e,f) their difference.

two Prediction and Research Moored Array in the Atlantic (PIRATA) moorings at 8°S, 30°W and 14°S, 32°W (Bourlès et al., 2008). Salinity at these buoy locations is typically available at four depths between 1 and 120 m. Finally, we examine water optical properties — specifically water turbidity using the monthly 9 km resolution 490 nm (blue-green wavelengths) diffusive attenuation coefficient data from the MODIS/TERRA satellite (oceandata.sci.gsfc.nasa.gov).

To monitor hydrologic processes we track rainfall using the monthly Global Precipitation Climatology Project (GPCP, version 2.2) rainfall, available at a 2.5° × 2.5° resolution (Adler et al., 2003). We track monthly continental discharge by combining discharge rates from the HYBAM observatory (www.ore-hybam.org) and the Brazilian water agency (www.ons.org.br/operacao/vazoes_naturais.aspx) to estimate the combined Amazon–Tocantins River discharge. We track daily surface winds from QuikSCAT (podaac.jpl.nasa.gov/dataset/QSCAT_LEVEL_3_V2) and Advanced SCATterometer (ASCAT), which are available at a 0.25° × 0.25° resolution (Bentamy & Croize-Fillon, 2012). Finally, we track monthly surface currents with the 1° × 1° OSCAR analysis (www.oscar.noaa.gov), and climatological monthly average currents, which are perhaps better represented by nearsurface drifter velocities (Lumpkin & Johnson, 2013).

3. Results

Near-surface salinity along the ship of opportunity transects extending northeastward from French Guiana shows the seasonal growth of the low salinity plume northward from the coast into the region of high salinity subtropical water as the calendar year progresses (Fig. 2a). This northward extension develops coincident with the seasonal increase in freshwater discharge by the Amazon and surrounding rivers and with the relaxation of onshore winds at the Amazon mouth (Fig. 3b). The multi-year time series of average SSS between 6°–15°N also reveals considerable year to year variability, for example with low SSS in 2005 and 2009 (Fig. 2b). The low values of SSS in 2009 occur in a year of above normal discharge (Fig. 3a, Foltz et al., 2012). In contrast, in 2005 the discharge was below normal (Fig. 3a, see Zeng et al., 2008 for analysis of the 2005 Amazon drought) but winds were also weaker than normal (Fig. 3b) suggesting that for this year a reduction in vertical exchange may have played the key role in the development of the plume. However the irregular shape of the plume and changes in the ship routes leave uncertainties in the correspondence of the TSG time series to plume salinity.

In view of the above examples illustrating SSS links with discharge and winds, the SSS difference between 2011 and 2012 is particularly intriguing. In contrast with stronger Amazon discharge in 2012 compared to 2011 (Fig. 3a) (and similar Orinoco discharge during the two years, not shown), the minimum salinity along the TSG transects shows a dramatic 1 psu salinification of the water from 2011 to 2012 (Fig. 2). The difference in SSS is explained in part by the difference in winds and related vertical mixing that were stronger in late spring through summer of 2012 (Fig. 3b). Fortunately for this recent period we have direct SSS observations from Aquarius and SMOS (Fig. 4). Although the two satellite SSS disagree on the sign of temporal changes of some

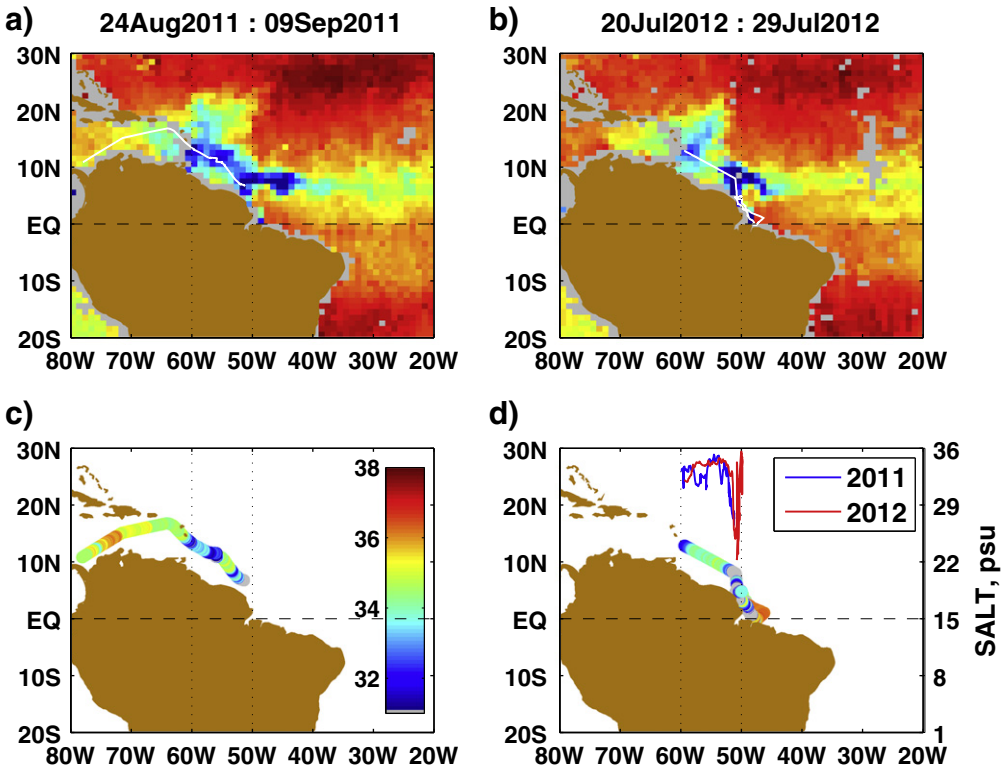

Fig. 5. (a,b) Aquarius SSS and cruise tracks (white) for 2011 and 2012. (c,d) In situ underway salinity along cruise tracks. Salinity colorbar in (c) applies to all panels. In situ salinity is also shown in (d) against the right hand axis for data collected between 60°W and 50°W. Gray is data gaps in (a,b) and SSS < 31 psu in (c,d).

large scale SSS patterns (in particular, in the north subtropical SSS maximum), these observations fortunately confirm the salinity increase over the plume area located northwest off the NBC retroflection from 2011 to 2012 (Fig. 4e,f). But, in the high gradient SSS region adjacent to the NBC retroflection and the western part of the NECC the SSS difference deducted from both products presents dipole-like patterns indicative of frontal shifts between the two years (Fig. 4e,f).

The increase in plume SSS is also apparent in the comparison of along-track SSS from the two ANACONDAS cruises in Aug–Sept 2011 and July 2012 Although the two cruise data were not collected at quite the same time of year, concurrent Aquarius SSS suggests that we should expect higher salinities during the second cruise than the first (Fig. 5a,b) and indeed this year to year difference is apparent in the in situ measurements (Fig. 5c,d), which show higher salinity taken along the coast between 60°W and 50°W in 2012 (Fig. 5d, inlay). Changes in Amazon (and Orinoco) discharge cannot explain the increase in salinity since discharge actually increased in 2012 (Fig. 3a). It should be noted that year to year changes in winds favor fresher SSS in 2011 due to weaker winds in spring–summer of 2011 compared to 2012. But impact of wind mixing on the plume characteristics is beyond the scope of this analysis. Here we consider a third explanation.

First we note that boreal spring rainfall was higher in 2011 than 2012 (Fig. 6a,c,e). The largest change between the two years occurs in coastal Brazil south of the equator and the adjacent ocean where areal average March–May (MAM) 2011 ocean rainfall exceeds 2012 MAM by 4 mm/day (3 mm/day), if averaging only positive (all) rainfall differences over the ocean within a 10°S–5°N, 50°W–15°W box, respectively (Fig. 6e). This coastal rainfall deficiency in 2012 is also reflected in a reduction in surface wind convergence along the coast (Fig. 6b,d) and implies that ocean rainfall delivered 1400 km^3 less fresh water to the southwestern tropical Atlantic in 2012 than in 2011. This reduction is equivalent to a 20% reduction of the annual cumulated Amazon discharge of about 6400 km^3 and is comparable to, or exceeds, interannual variations in Amazon discharge. A simple mixed layer salt budget indicates that a 4 mm/day rainfall reduction for 3 months would enhance local salinity of the upper 20 m (see Hu et al., 2004 for the vertical scale in the salinity range 30–35 psu) by about 0.9 psu. This effect alone might explain the observed magnitude of interannual change in SSS shown (Fig. 4e,f).

The dilution by enhanced 2011 MAM rainfall in the southwestern tropical Atlantic (Fig. 6e) is seen in the SMOS SSS difference between the two years averaged over two months (May–June) following the peak of spring rainfall (Fig. 6f). But, in contrast to rainfall anomaly present mostly west of 15°W, the fresh SSS anomaly extends across the entire basin between the equator and 10°S suggesting that westward freshwater transport by the South Equatorial Current out of the Gulf of Guinea might play a role. The May–June SSS difference also doesn't reveal an expected dilution by enhanced ocean rainfall off the equatorial Brazil coast (Fig. 6e,f), but rather a strong jet of the NBC may cause a non-local SSS response.

Longer records from the 8°S, 30°W PIRATA mooring evidence the dilution by enhanced rainfall in the southwestern tropical Atlantic in 2009 and 2011 (Fig. 7a. The mooring location is marked on Fig. 6e). At this location the freshening peaks by early boreal summer in response to boreal spring rainfall. The strongest fresh event in the 2005–2013 records occurs in 2009 in response to an anomalous southward shift of the ITCZ forced by the cold north tropical Atlantic that year (see Foltz et al., 2012 for the 2009 analysis). The 2011 fresh event also develops in response to above normal rainfall (Fig. 6e). But, in contrast with the 2009 event the 2011 freshening is not linked with the Atlantic SST and may be linked to the eastern equatorial Pacific SST, which was colder than normal in 2011 (not shown). Some of the freshened water observed at 8°S, 30°W is advected southwestward by the South Equatorial Current (Fig. 1) so that it arrives at the 14°S, 32°W mooring 4 months later (Fig. 7b). But most of the freshened water should be transported towards the coast and then northwestward

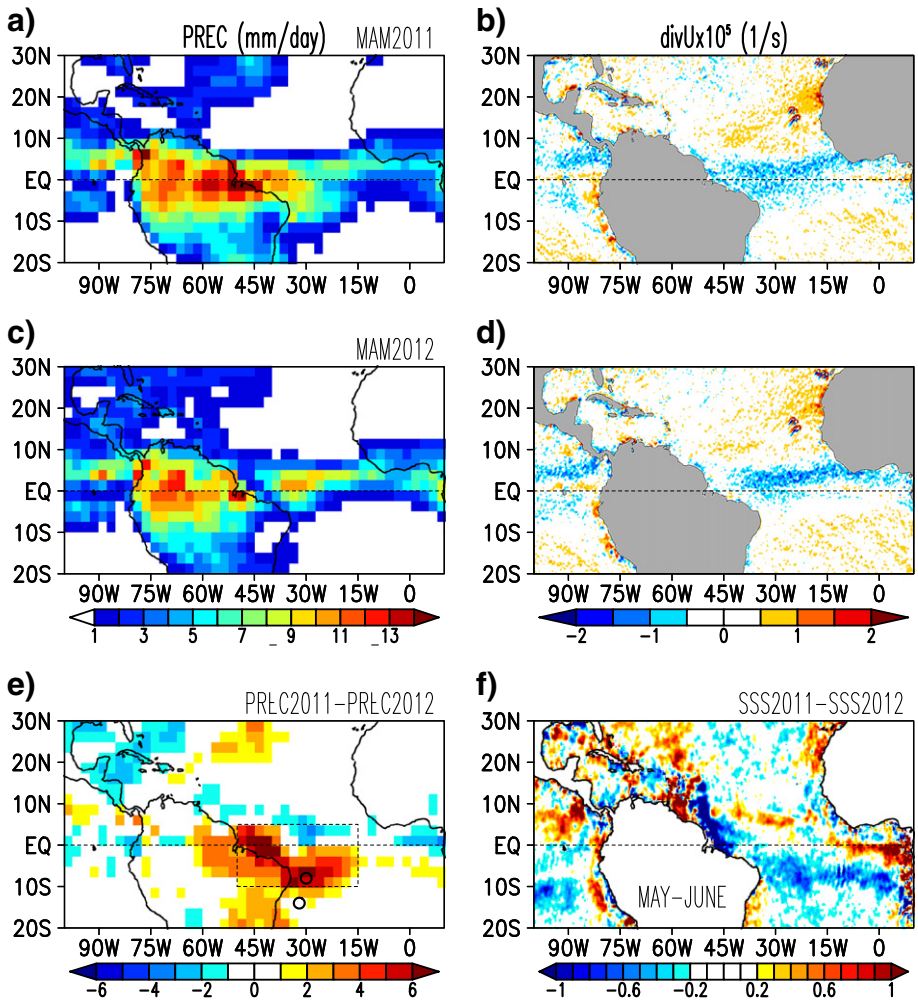

Fig. 6. Precipitation averaged March–May (MAM) of (a) 2011, (c) 2012, and (e) their difference. ASCAT wind divergence averaged MAM of (b) 2011, and (d) 2012. The 8°S, 30°W and 14°S, 32°W PIRATA mooring locations and area for the ocean rainfall averaging are shown in (e). (f) SMOS SSS difference (psu) during months following MAM rainfall.

along the coast by the NBC (as evidenced by local currents in Fig. 1), reducing the salinity of the Amazon plume.

Ocean currents, including eddies, play a key role in shaping the spatial extent of the plume by transporting the fresh waters thousands of miles away from the river mouth. Fig. 8b, d, and f illustrate the surface currents averaged over the time interval extending from the maximum Amazon discharge in May–June through the maximum plume areal extent in September. Incidentally, while the currents in this region are strongly seasonal the OSCAR surface current product suggests significant differences between June–September currents in 2011 and 2012 due to related differences in sea level (not shown). In particular, the northwestward transport of Amazon water along the coast by the NBC is stronger and more variable in 2011, but the retroflection is stronger in 2012 (Fig. 8b,d).

The difference in currents probably contributes to the 2012/2011 difference in the plume dispersal, which is seen in the ocean color (Fig. 8a,c). Ocean color in the western tropical Atlantic correlates with SSS (Salisbury et al., 2011) because the two are affected by the continental discharge. The fate of continental discharge depends on the horizontal transport and dispersal by ocean currents. In fact, stronger and more variable transport along the coast by the NBC in 2011 results in higher diffusive attenuation coefficient at 490 nm (KD490) northwestward of the retroflection area, while KD490 is higher in the NECC east of 45°W in 2012. Diffusive attenuation was even higher northwestward of the retroflection area in 2009 when both currents and continental discharge were strong.

Using historical TSG observations (Fig. 2) and ocean surface currents (Fig. 8) we select years differing by environmental factors affecting the plume. In line with the record low SSS evident in TSG transects (Fig. 2), the 2009 KD490 in the fresh pool area is the highest among the three years (Fig. 8). Low SSS in 2009 results from the combination of relatively strong NBC (Fig. 8f) and above normal Amazon discharge (Fig. 3a). To illustrate an impact of the continental discharge we compare the 2009 and 2011 data. During these two years the NBC northwestward of the retroflection area was similarly strong (Fig. 8b,f). Indeed, between January and September the cumulative discharge was 6330 km^3 in 2009 reducing to 5650 km^3 in 2011 (Fig. 3a). This extra 680 km^3 of fresh water available in 2009 would result in a fresh anomaly of 1.2 psu in the upper 20 m over an area of 10^6 km^2. In contrast, the 2012 January–September integrated discharge was 5980 km^3 or 330 km^3 more than in 2011. Yet, despite the increase in discharge, the plume SSS was almost 1 psu saltier (Figs. 2, 4)! This difference is attributed to the difference in the surface currents, but leaving room for other mechanisms.

Year-to-year SSS variations last and have implications for SSS climate, since SSS is not damped like SST (e.g. Foltz & McPhaden, 2008). Because anomalies of SSS do not directly enter air–sea feedbacks in the way that anomalies of SST do, it is perhaps not surprising for such SSS anomalies to persist in the tropical Atlantic for many months. Anomalous SSS

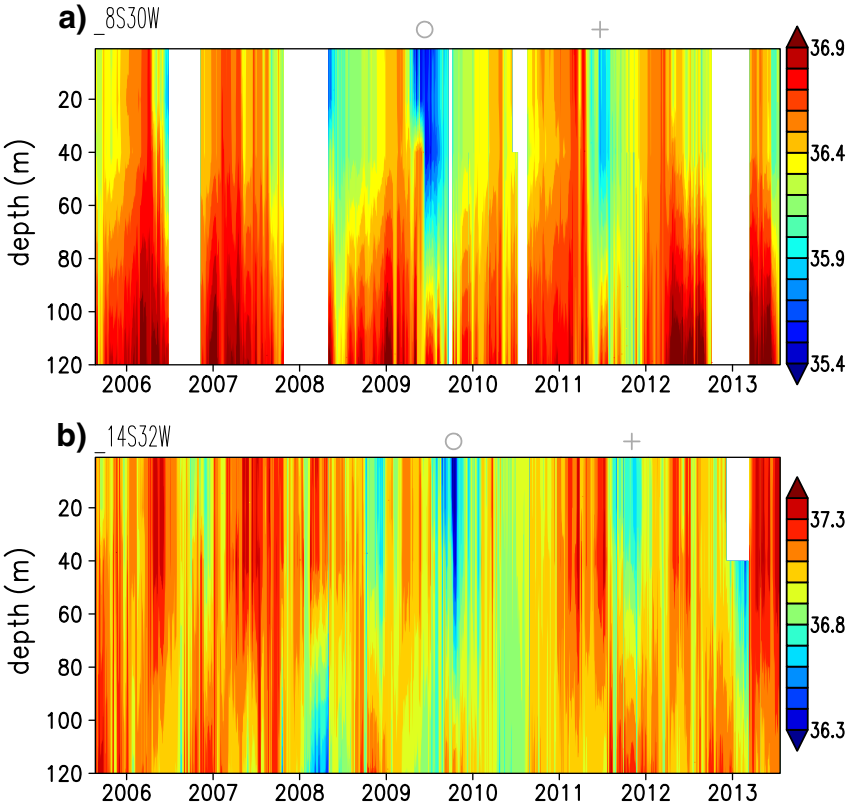

Fig. 7. Daily salinity (psu) with time and depth at the (a) 8°S, 30°W and (b) 14°S, 32°W PIRATA moorings. The 2009 and 2011 fresh events are marked with 'o' and '+', respectively.

(referenced to the seasonal cycle evaluated with the first two annual harmonics) reveals a long-lived pattern of fresh SSS east of the Lesser Antilles (Fig. 9a). Computing anomalies using time records that are only two years long essentially focuses on the difference between conditions during the two years. This indicates that the fresh SSS anomaly that originated in 2011 was present in the region through boreal spring of 2012 (Fig. 9b). During this period the SSS anomaly was about 0.5 psu fresher than during the corresponding period of the next year. We still have to understand the fate of the Amazon fresh anomalies, their life span, and impacts on the thermo-haline properties of the tropical/subtropical Atlantic.

4. Summary

New satellite SSS observations from the Aquarius/SACD satellite and in situ thermosalinograph measurements from commercial ships reveal significant year-to-year variations in the salinity of the Amazon/Orinoco plume, which was about 1 psu saltier in late summer–early fall of 2012 relative to 2011. The variability seen by Aquarius is also apparent in observations from the SMOS satellite (not shown). This increase in salinity is surprising because continental discharge was stronger in 2012 than in 2011 as evident in both discharge time series and satellite turbidity observations, while the surface winds (hence their mixing impact) were mostly similar in these two years. It turns out that the most striking difference is the reduction in rainfall over the ocean to the southeast of the plume and weaker coastal currents which bring this freshwater to the region of the plume. We propose that changes in rainfall over the ocean to the southeast of the plume in boreal spring and its transport can substantially impact the salinity of the plume in boreal fall. Exploitation of this property may help seasonal predictions of the intensity of fall hurricanes.

This paper leaves behind at least two important aspects that might be relevant to the plume dynamics. One aspect involves impacts of winds on the vertical mixing and thus the depth of barrier layer and surface salinity. Another aspect involves possible impacts of the residual conditions in the region from the previous year that might be important for setting surface salinity.

Our record of satellite measurements of SSS is still quite limited and it may be some years before we know how unusual it is for the salinity of the Amazon/Orinoco plume to change from year to year due to ocean rainfall. However, coupled climate models, which contain all of the physical processes described above, may provide some guidance on these points.

Acknowledgments

This research was supported by NASA (NNX12AF68G, NNX09AF34G, and NNX10AO99G). GR was supported by CNRS with grants from CNES for SMOS validation studies. VC was supported by NSF (OCE-0933975) and the Gordon and Betty Moore Foundation. The continental discharge data are provided by the HYBAM observatory and the Brazil Water Agency. The GOSUD data used here are from the MN Colibri and Toucan, two vessels equipped and maintained by ORE SSS. We are grateful to Denis Diverres (US IMAGO, IRD) for maintaining the tropical Atlantic TSG network and validating the data. The LOCEAN_v2013 SSS has been produced by LOCEAN/IPSL that participates in the Ocean Salinity Expertise Center (CECOS) of Centre Aval de Traitemenent des Donnees SMOS (CATDS).

References

Adler, R. F., Huffman, G. J., Chang, A., Ferraro, R., Xie, P. P., Janowiak, J., et al. (2003). The version-2 global precipitation climatology project (GPCP) monthly precipitation analysis (1979–present). *Journal of Hydrometeorology, 4*, 1147–1167. http://dx.doi.org/10.1175/1525-7541(2003)004<1147:TVGPCP>2.0.CO;2.

Amarasekera, K. N., Lee, R. F., Williams, E. R., & Eltahir, E. (1997). ENSO and the natural variability in the flow of tropical rivers. *Journal of Hydrology, 200*(1–4), 24–39.

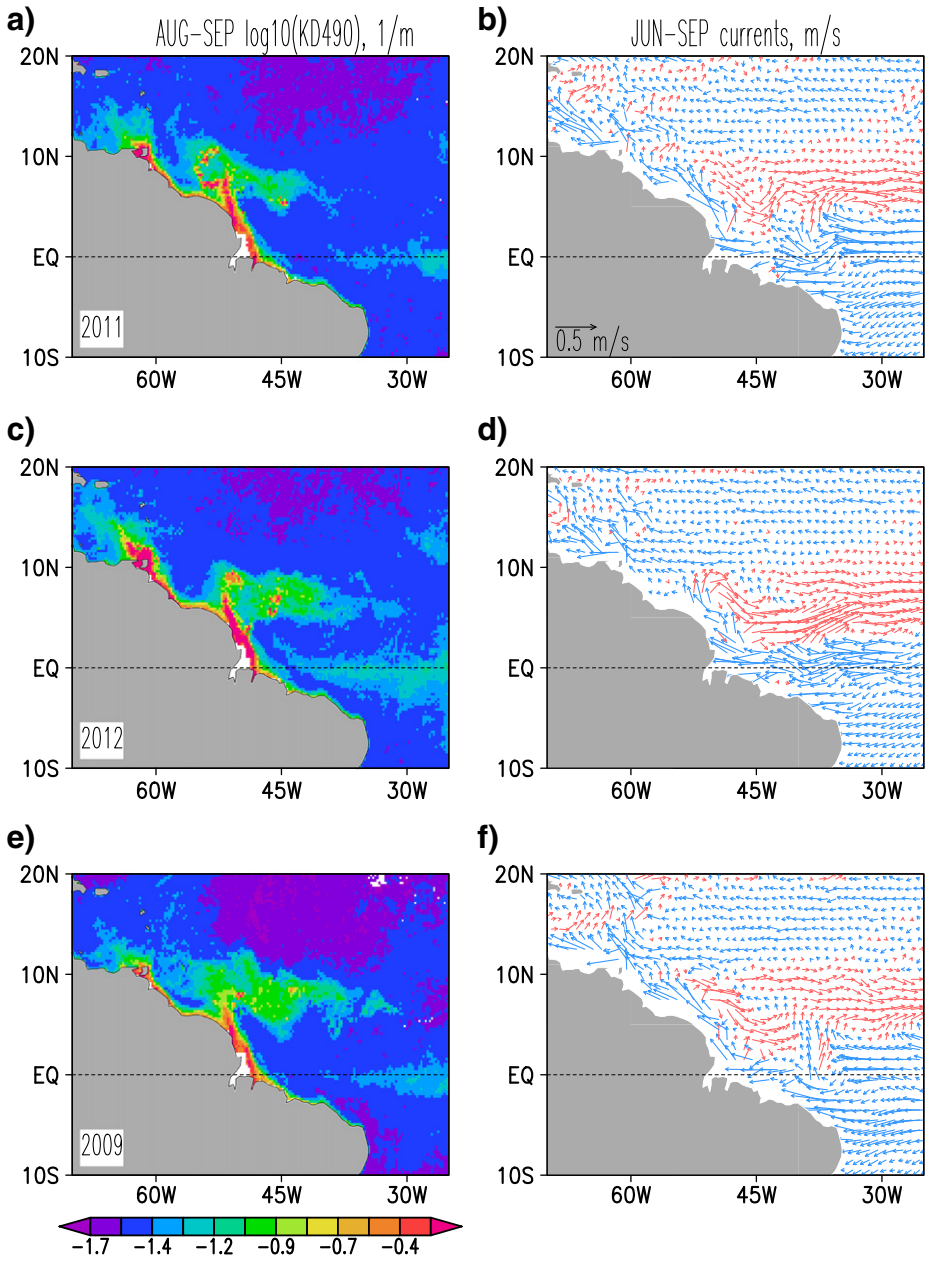

Fig. 8. Diffusive attenuation coefficient at 490 nm (KD490) in August–September of (a) 2011, (c) 2012, and (e) 2009. (b,d,f) Surface currents in June–September of corresponding years. Eastward/westward currents are in red/blue, respectively.

Balaguru, K., Chang, P., Saravanan, R., Leung, L. R., Xu, Z., Li, M., et al. (2012). Ocean barrier layers' effect on tropical cyclone intensification. *PNAS*. http://dx.doi.org/10.1073/pnas.1201364109.

Bentamy, A., & Croize-Fillon, D. (2012). Gridded surface wind fields from Metop/ASCAT measurements. *International Journal of Remote Sensing*, *33*, 1729–1754.

Bourlès, B., Lumpkin, R., McPhaden, M. J., Hernandez, F., Nobre, P., Campos, E., et al. (2008). The Pirata Program: History, accomplishments, and future directions. *Bulletin of the American Meteorological Society*, *89*, 1111–1125.

Boutin, J., Martin, N., Reverdin, G., Yin, X., & Gaillard, F. (2013). Sea surface freshening inferred from SMOS and ARGO salinity: Impact of rain. *Ocean Science*, *9*, 183–192. http://dx.doi.org/10.5194/os-9-183-2013.

Boyer, T. P., Levitus, S., Antonov, J. I., Reagan, J. R., Schmid, C., & Locarnini, R. (2012). [Subsurface salinity] Global oceans [in State of the Climate in 2011]. *Bulletin of the American Meteorological Society*, *93*(7), S72–S75.

Carton, J. A., & Katz, E. J. (1990). Estimates of the zonal slope and seasonal transport of the Atlantic North Equatorial Countercurrent. *Journal of Geophysical Research*, *95*, 3091–3100. http://dx.doi.org/10.1029/JC095iC03p03091.

Chen, J. L., Wilson, C. R., & Tapley, B.D. (2010). The 2009 exceptional Amazon flood and interannual terrestrial water storage change observed by GRACE. *Water Resources Research*, *46*(12), W12526. http://dx.doi.org/10.1029/2010WR009383.

Dessier, A., & Donguy, J. R. (1994). The sea surface salinity in the tropical Atlantic between 10°S and 30°N — Seasonal and interannual variations (1977–1989). *Deep Sea Research I*, *41*, 81–100.

Ffield, A. (2007). Amazon and Orinoco River plumes and NBC rings: Bystanders or participants in hurricane events? *Journal of Climate*, *20*, 316–333.

Foltz, G. R., & McPhaden, M. J. (2008). Seasonal mixed layer salinity balance of the tropical North Atlantic Ocean. *Journal of Geophysical Research*, *113*, C02013. http://dx.doi.org/10.1029/2007JC004178.

Foltz, G. R., McPhaden, M. J., & Lumpkin, R. (2012). A strong Atlantic Meridional Mode event in 2009: The role of mixed layer dynamics. *Journal of Climate*, *25*, 363–380. http://dx.doi.org/10.1175/JCLI-D-11-00150.1.

Grodsky, S. A., Reul, N., Lagerloef, G. S. E., Reverdin, G., Carton, J. A., Chapron, B., et al. (2012). Haline hurricane wake in the Amazon/Orinoco plume: AQUARIUS/SACD and SMOS observations. *Geophysical Research Letters*, *39*, L20603. http://dx.doi.org/10.1029/2012GL053335.

Hellweger, F. L., & Gordon, A. L. (2002). Tracing Amazon River water into the Caribbean Sea. *Journal of Marine Research*, *60*, 537–549. http://dx.doi.org/10.1357/002224002762324202.

Hu, C., Montgomery, E. T., Schmitt, R. W., & Muller-Karger, F. E. (2004). The dispersal of the Amazon and Orinoco River water in the tropical Atlantic and Caribbean Sea: Observation from space and S-PALACE floats. *Deep Sea Research II*, *51*, 1151–1171.

Aquarius salinity validation analysis. Lagerloef, G. (Ed.). (2013). *Aquarius Project document: AQ-014-PS-0016, 18 February 2013, Data Version 2.0* (ftp://podaac-ftp.jpl.nasa.gov/allData/aquarius/docs/v2/AQ-014-PS-0016_AquariusSalinityDataValidationAnalysis_DatasetVersion2.0.pdf)

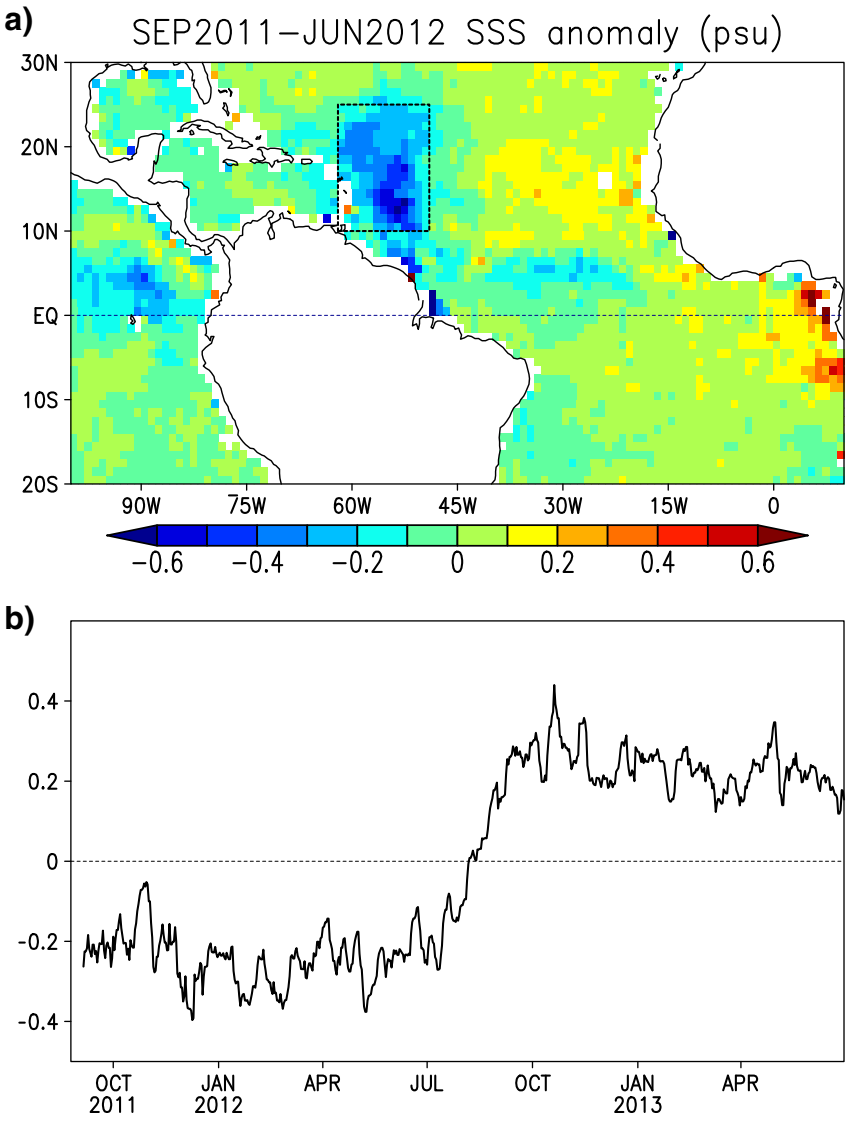

Fig. 9. (a) Anomalous Aquarius SSS averaged September 2011 through June 2012. (b) Time series of anomalous SSS averaged over the box shown in (a).

Lagerloef, G., Wentz, F., Yueh, S., Kao, H. -Y., Johnson, G. C., & Lyman, J. M. (2012). Aquarius satellite mission provides new, detailed view of sea surface salinity, in State of the Climate 2011. *Bulletin of the American Meteorological Society*, *93*(7), S70–S71.

Lentz, S. J. (1995). Seasonal variations in the horizontal structure of the Amazon Plume inferred from historical hydrographic data. *Journal of Geophysical Research*, *100*(C2), 2391–2400. http://dx.doi.org/10.1029/94JC01847.

Lumpkin, R., & Johnson, G. C. (2013). Global ocean surface velocities from drifters: Mean, variance, El Niño–Southern Oscillation response, and seasonal cycle. *Journal of Geophysical Research*, *118*. http://dx.doi.org/10.1002/jgrc.20210.

Mignot, J., Lazar, A., & Lacarra, M. (2012). On the formation of barrier layers and associated vertical temperature inversions: A focus on the northwestern tropical Atlantic. *Journal of Geophysical Research*, *117*, C02010.

Muller-Karger, F. E., McClain, C. R., & Richardson, P. L. (1988). The dispersal of the Amazon's water. *Nature*, *333*, 56–58.

Nikiema, O., Devenon, J. -L., & Baklouti, M. (2007). Numerical modeling of the Amazon River plume. *Continental Shelf Research*, *27*(7), 873–899. http://dx.doi.org/10.1016/j.csr.2006.12.004.

Ropelewski, C. F., & Halpert, M. S. (1987). Global and regional scale precipitation patterns associated with the El Niño/Southern Oscillation. *Monthly Weather Review*, *115*, 1606–1626. http://dx.doi.org/10.1175/1520-0493(1987)115<1606:GARSPP>2.0.CO;2.

Salisbury, J., Vandemark, D., Campbell, J., Hunt, C. W., Wisser, D., Reul, N., et al. (2011). Spatial and temporal coherence between Amazon River discharge, salinity, and light absorption by colored organic carbon in western tropical Atlantic surface waters. *Journal of Geophysical Research*, *116*, C00H02.

Satyamurty, P., da Costa, C. P. W., Manzi, A. O., & Candido, L. A. (2013). A quick look at the 2012 record flood in the Amazon Basin. *Geophysical Research Letters*, *40*. http://dx.doi.org/10.1002/grl.50245.

Tzortzi, E., Josey, S. A., Srokosz, M., & Gommenginger, C. (2013). Tropical Atlantic salinity variability: New insights from SMOS. *Geophysical Research Letters*. http://dx.doi.org/10.1002/grl.50225.

Xie, S. -P., & Carton, J. A. (2004). In C. Wang, S. P. Xie, & J. A. Carton (Eds.), *Tropical Atlantic variability: Patterns, mechanisms, and impacts, in earth's climate*. Washington, DC: American Geophysical Union. http://dx.doi.org/10.1029/147GM07.

Yin, X., Boutin, J., & Spurgeon, P. (2012). First assessment of SMOS data over open ocean: Part I Pacific Ocean. *IEEE Transactions on Geoscience and Remote Sensing*. http://dx.doi.org/10.1109/TGRS.2012.2188407.

Zeng, N., Yoon, J., Marengo, J., Subramaniam, A., Nobre, C., Mariotti, A., et al. (2008). Causes and impacts of the 2005 Amazon drought. *Environmental Research Letters*, *3*, 014002. http://dx.doi.org/10.1088/1748-9326/3/1/014002.